

CHAPTER IV

RESULTS AND DISSCUSION

In this study, AAm/CA hydrogels were prepared by free radical polymerization in aqueous solutions of AAm, CA and the crosslinker NMBA in the presence of gas bubbles. Carbon dioxide gas bubbles were generated by a reaction of sodium bicarbonate with the acid solution of CA. The amount of foam was governed by the amount of acid in the reaction mixture. We used an excess amount of sodium bicarbonate so that the foam size and amount were controlled by amount of added acid, which was CA in this case. CA thus functions as a comonomer and a foam accelerator. During the crosslinking polymerization, the viscosity of the medium increased gradually. The increased viscosity slowed down the bubble formation.

The foam stabilizer used in the present work is considered as one of the foaming materials with the best properties. Polyoxyethylene/polyoxypropylene/polyoxyethylene block copolymer (LF[®] 127), has the best foaming properties for most hydrophilic monomers; that is, it sustains the foam or bubbles for the longest period of the time. In addition, it functions as a surface crosslinking agent, enhancing liquid permeability, improving the water absorption rate, and increasing water absorption capacity (33).

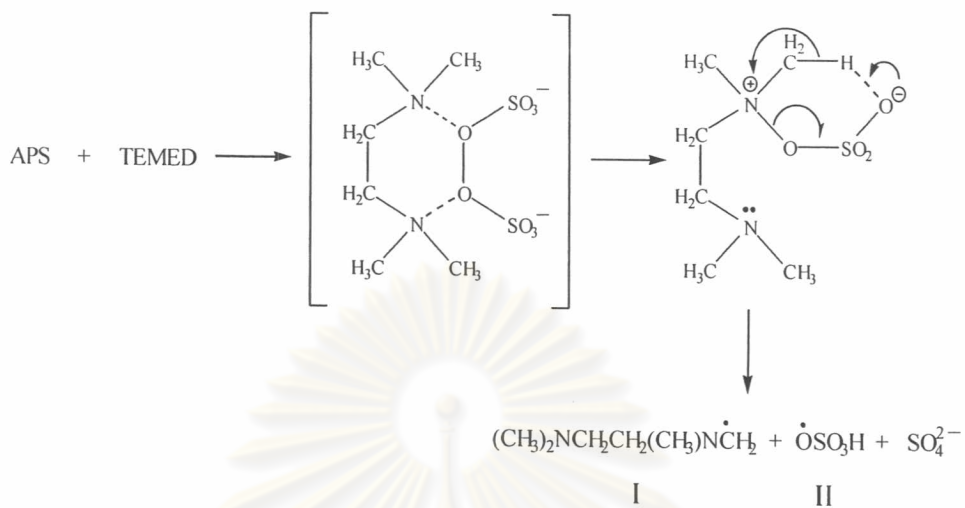
The polymerization started from carbon dioxide gas generated from the reaction of crotonic acid and sodium bicarbonate. When NaHCO₃ powder was added into the solution, followed immediately by the LF[®] 127 foam stabilizer. The bubbles

were accommodated by the monomers, initiator radicals and crosslinker. The initial polymerization should take place in the gaseous phase from which the clean and unique polymer chains were produced.

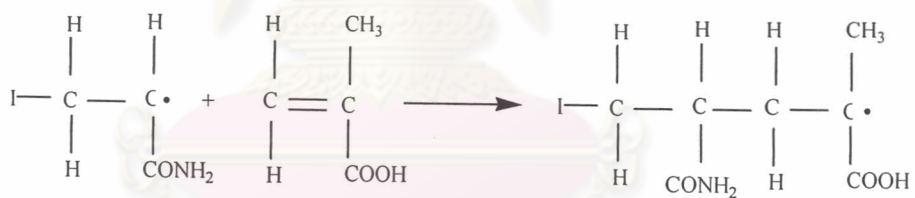
After the bubbles had been destabilized, they fell into the solution. Afterward, the crosslinking polymerization was continued in the aqueous phase until a foamed superabsorbent polymer was achieved. The foamed polymerization could possibly be depicted as a combined polymerization of bulk polymerization and solution polymerization. In the polymerization, first step is a reaction between APS and TEMED in which the TEMED molecule is left with an unpaired valence electron. The activated TEMED molecules can combine with an AAm and CA comonomer or crosslinker molecules, in the process the unpaired electron is transferred to the monomeric units, so that they in turn become reactive. The polymer (AAm) or copolymer (AAm/CA) can grow continuously and indefinitely with an active center being continually shifted to the free end of the chain. Crosslinker molecules can be incorporated into chains simultaneously and forms a permanent link between them.

Polymerization and crosslinking reaction has taken place for half an hour to achieve the AAm/CA gelation. The crosslinked copolymer is colorless and some of them are semi-transparent. They are soft and elastic with a slippery touch on a delicate surface. The possible free radical polymerization of poly[acrylamide/(crotonic acid)] is shown in Figure 4.1.

Initiation



Copolymerization



ศูนย์วิทยทรัพยากร
 จุฬาลงกรณ์มหาวิทยาลัย

Crosslinking

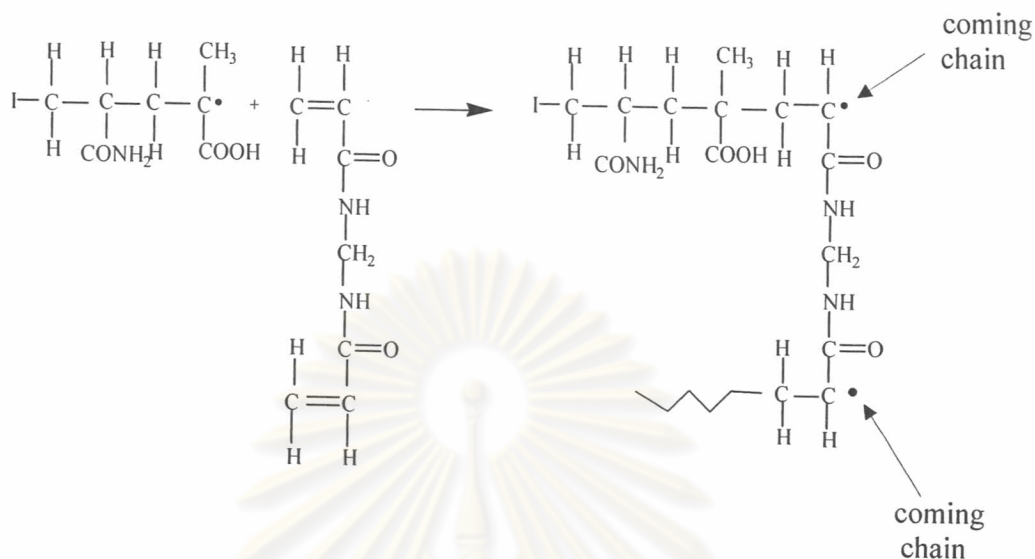


Figure 4.1 Possible copolymerization and crosslinking reaction mechanism between acrylamide and crotonic acid monomer with a N-MBA crosslinker.

4.1 Effect of Crotonic Acid Concentration

The result on water absorbency of the copolymers synthesized by crosslinking polymerization with various mole percents of crotonic acid is shown in Table 4.1 and Figure 4.2.

ศูนย์วิทยทรัพยากร
จุฬาลงกรณ์มหาวิทยาลัย

Table 4.1 Effect of crotonic acid concentration (mole percent) on water absorbency (Q) of the synthesized copolymers*

Crotonic acid (mole percent)	Water absorbency (Q) g g ⁻¹
0	54±4
1	104±2
2	111±7
3	110±2
4	110±4
5	112±9
7	111±2
10	113±5
15	120±4
20	123±7
30	130±4

*Polymerization reactions were carried out at 1% APS, 2% TEMED, 1% N-MBA,

7% LF[®]127, 28% NaHCO₃, 250 rpm, 50°C and 30 min.

ศูนย์วิทยาศาสตร์
จุฬาลงกรณ์มหาวิทยาลัย

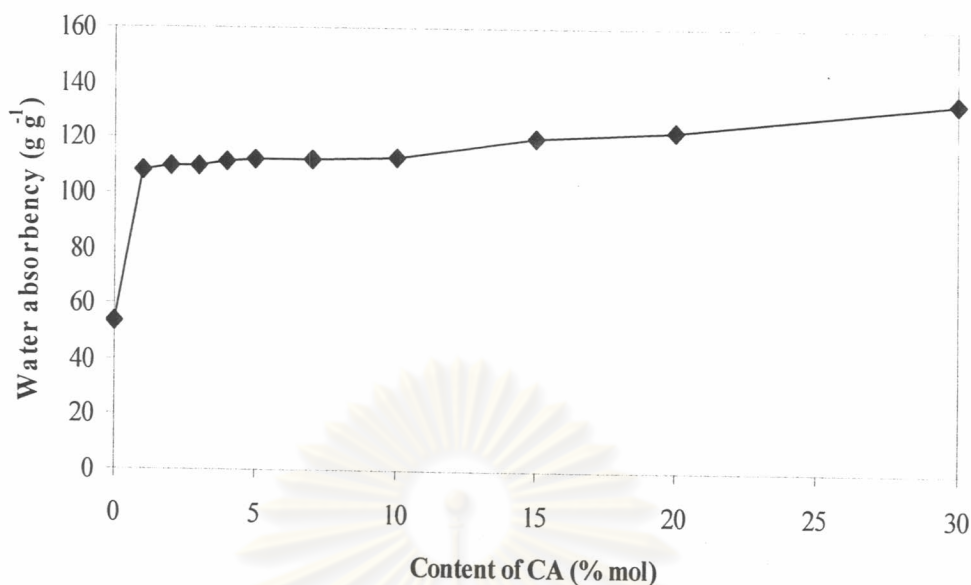


Figure 4.2 Effect of crotonic acid concentration (mole percent) on the water absorbency (Q) of the synthesized copolymer at 1% APS, 2% TEMED, 1% N-MBA, 7% LF[®]127, 28% NaHCO₃, 250 rpm, 50°C and 30 min.

The synthesized copolymers of acrylamide (AAM) and crotonic acid (CA) are swollen in water on the account of the hydrophilic pendants (amide and carboxylic groups) in their structure, especially the synthesized copolymer, which content of crotonic acid comonomer at 30% mol produced the high water absorbency value of 130 ± 4 times its dry weight. The values of water absorbency of polyacrylamide (PAM) is 54 ± 4 times its dry weight, but the values of water absorbency of P(AAM-co-CA) hydrogel vary between 104 ± 2 and 130 ± 4 times its dry weight. Comparing the radical copolymerization of AAM(M_1)-CA(M_2) with $r_1 = 4.72$ and $r_2 = 0.11$ (34), crotonic acid do not like to self-polymerize to obtain the homopolymer. Thus the increasing homopolymer content may be from the formation of polyacrylamide or the random

copolymerization of AAm and CA radicals. However in a chain crosslinking copolymerization, the reactivity of crosslinking agent must also be considered. The r_1 and r_2 values for the system of AAm/N-MBA are 0.64 and 1.77 respectively (35). A large tendency of the crosslinking comonomer to react with itself is generally observed. However, unless steric effects can prevent the self-polymerization of N-MBA, then AAm prefers to react with N-MBA to give a random type of copolymer or a crosslinked polymer. As a consequence, N-MBA tends to form sequences longer than other one even with low contents of N-MBA.

It is well known that the swelling of hydrogel is induced by the electrostatic repulsion of the ionic charges of its network. The ionic charge content in the polymeric structure is important. The superabsorbent polymer containing crotonic acid contains many hydrophilic units (-COOH) and the swelling of the polymer increases due to an increase of the hydrophilicity. The number of hydrophilic groups of AAm/CA copolymers is higher than that in the polyacrylamide, so the swelling of AAm/CA copolymers is much higher (20, 29, 30). We found that the superabsorbent polymer is a viscous gel. We anticipated that AAm moiety could contribute to chain stiffness due to its relatively hydrophobic nature compared to that of CA. The hydrophobicity of AAm contributes to the gel strength of the superabsorbent polymer. Also, N-MBA provides the crosslinking reaction to CA portion. We need to mention that the pre-neutralization of crotonic acid was not performed before polymerization because the ionized monomer reacts more slowly in the propagation step of polymerization. Higher percentages of the soluble polymer and higher residual monomer concentrations in the final product can evidence. Because an excess amount of sodium bicarbonate was used as a foaming agent, one must consider that

there is sodium bicarbonate left in the reaction solution, which can neutralize CA to become sodium crotonate, which is very water soluble (36).

Flory described the mechanism of swelling of an ionic network (37). If the polymer chains making up the network contain ionizable group, the swelling forces may be greatly increased as a result of the localization of the charges on the polymer chains. When the crosslinked copolymer is neutralized with sodium hydroxide, the negatively charged carboxyl groups attached to the polymer chains set up an electrostatic repulsion, which tend to expand the network. Sodium ions, which screen the negative charges of carboxyl groups, reduce the electrostatic repulsion tremendously, leading to the decrease in water absorption. The water absorbency of synthesized copolymer depends not only on the mole ratio of CA, but also on the degree of neutralization of CA.

The water absorbency of the superabsorbent polymers containing 2 and 10 mole percents was selected for further investigation because the water absorbency values were almost constant at higher mole percents. Further increases in crotonic acid concentration did not justify the significant increase in water absorbency.

4.2 Effect of APS/TEMED Concentration

The water absorbency of the crosslinked copolymers synthesized with various initiator (APS/TEMED) concentrations for the solution polymerization is shown in Table 4.2 and Figure 4.3 .

Table 4.2 Effect of the initiator concentration on water absorbency (Q) of the synthesized copolymers*

Content of APS (%wt)	Water absorbency (Q) g g ⁻¹	
	AAm/CA: 98/2	AAm/CA : 90/10
0.5	105±11	88±9
1.0	110±2	113±3
1.5	109±2	110±3
2.0	105±3	99±3

*Polymerization reactions were carried out at 2% TEMED, 1% N-MBA, 7% LF[®]127, 28% NaHCO₃, 250 rpm, 50°C and 30 min.

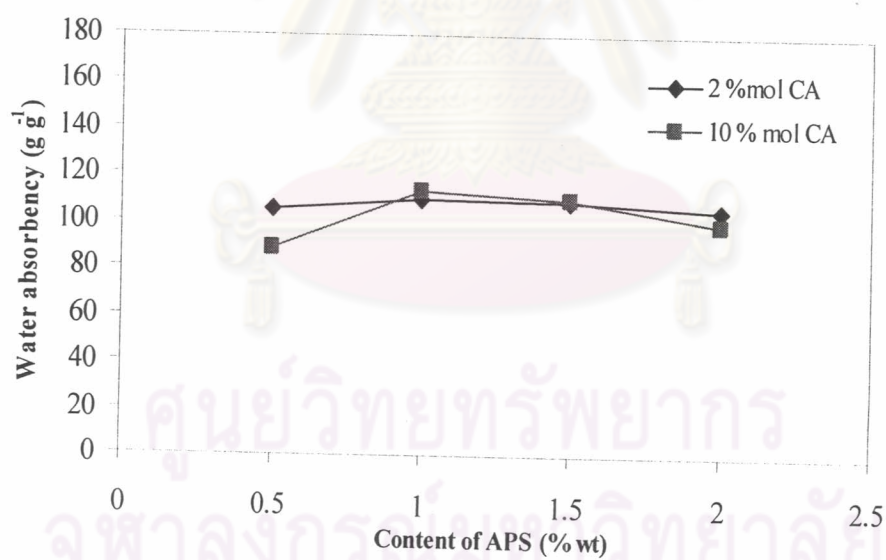


Figure 4.3 Effect of initiator concentration on the water absorbency (Q) of the synthesized copolymer at 2% TEMED, 1% N-MBA, 7% LF[®]127, 28% NaHCO₃, 250 rpm, 50°C and 30 min.

Water absorbency increases linearly with an increase in the initiator of 1.0% wt. and then slightly decreases with increasing initiator content. As mentioned above, the rate of polymerization depends on the concentration of monomers and initiator radicals in a bimolecular termination. When APS and TEMED are used as a redox initiator pair for the free radical polymerization, the free radical (I), *N,N,N',N'* tetramethylethylenediamide radical, is one of the initial free radicals responsible for the initiation of vinyl polymerization in addition to sulfate free radical (II). The mechanism representing the production of initial radicals for the polymerization is shown in Figure 4.1.

This redox initiation pair produces two radicals, which may be claimed to be responsible for the fast polymerization. At the higher APS concentrations (1.5 and 2.0% wt.), too many radicals were produced, resulting in an abundance of short kinetic chains, in which the superabsorbent polymers had lower molecular weights. This inevitably reduced the swelling capacity. The TEMED accelerated the generation of a higher amount of free radicals to produce the shorter kinetic chains and/or radical recombination.

4.3 Effect of *N,N'*-methylenebisacrylamide Concentration

The water absorbency of the superabsorbent polymers, synthesized by 2 and 10 mole percent of AAm/CA with 1% wt. APS, 2% wt. TEMED and various concentrations of the N-MBA crosslinking agent is shown Table 4.3 and Figure 4.4.

Table 4.3 Effect of concentration of crosslinking agent on the water absorbency (Q) of the synthesized copolymer*

Content of N-MBA (%wt)	Water absorbency (Q) g g ⁻¹	
	AAm/CA: 98/2	AAm/CA : 90/10
0.5	211±9	129±6
1.0	110±2	113±3
1.5	104±5	108±2
2.0	82±7	104±1

*Polymerization reactions were carried out at 1.0% APS, 2% TEMED, 7% LF[®]127, 28% NaHCO₃, 250 rpm, 50°C and 30 min.

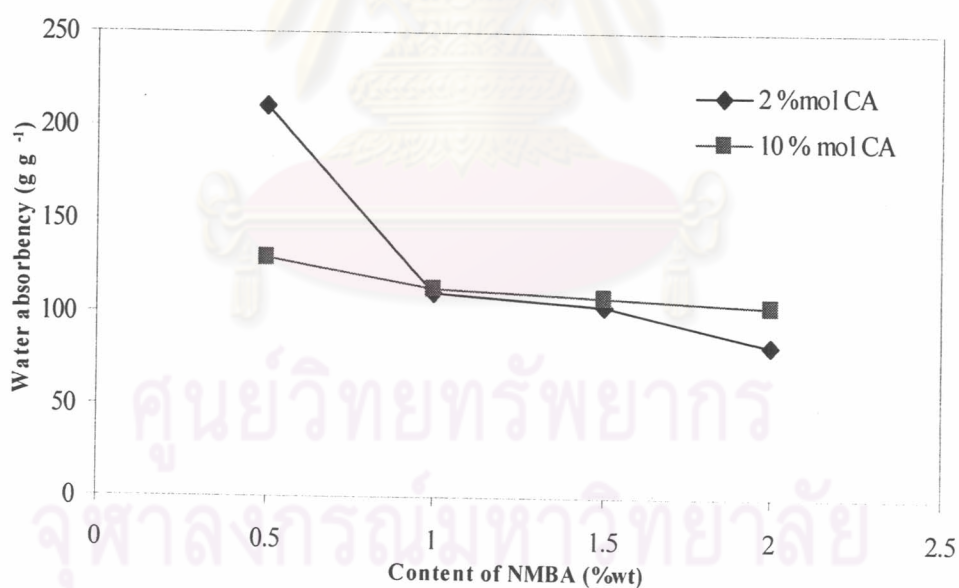


Figure 4.4 Effect of crosslinking agent concentration on the water absorbency (Q) of the synthesized copolymer at 1.0% APS, 2% TEMED, 7% LF[®]127, 28% NaHCO₃, 250 rpm, 50°C and 30 min concentration.

The relationship between water absorbency and crosslinking agent N-MBA is illustrated in Figure 4.4. In the presence of high crosslinking agent concentrations, more crosslinks can be formed to give rigid chains that reduce swelling of the gel as well.

Additionally, we did not extract the soluble part (non-crosslinked moiety) of the polymer before carrying out the water absorption experiment. The soluble portion is anticipated to interfere with the extent of water absorption in a negative way. Buchholz (38) reported that the solubility of a crosslinked polymer depended on the extent of neutralization, which could exhibit different effectiveness in the crosslinked products. In general, crosslinking agents have been employed to improve the strength of the swollen gel but they very effectively reduce water absorbency if too high a crosslinking agent concentration is used. Synthesis route of the copolymer by free radical copolymerization using the redox initiator pair with N-MBA crosslinking agent is shown in Figure 4.1.

Table 4.4 and Figure 4.5 show the number-average molar mass between crosslinks and crosslinking density of the synthesised poly(AAm-co-CA) by varying the N-MBA concentration range of 0.5 to 2% wt., based on the monomer content. The hydrogels containing more CA moities swell more than the others. Increasing the crosslinking agent concentration increases the crosslinking density, reduces the swelling of gel because of obtained rigid gel as seen in Figure 4.4. The values of the crosslinking density are related owing to the values of the number-average molar mass between crosslinks. Increasing the crosslinking agent concentration decrease the \bar{M}_c between the two main backbones. The larger the \bar{M}_c indicates the longer chains

between the two backbones. The results obtained show that the \bar{M}_c values are affected by the amount of crotonic acid. With an increasing concentration of crotonic acid in the copolymeric structure, the \bar{M}_c values increased. Ionic content dependence of elastic behavior originates from the variation of the extent of cyclization reactions depending on the charge density of polymer coil. According to this approach, as the ionic content of the polymer increases, the growing chains in the pregel regime will assume an extended conformation. This will result in a decrease of cyclic formation reactions because of the thermodynamic excluded volume effect and therefore will increase the \bar{M}_c values of the final hydrogel (39). With cyclization, the cycle is formed when the macroradical attacks the pendent vinyl groups in the same kinetic, while with multiple crosslinking, it is formed if the radical attacks double bonds pendant on other chains already chemically connected with the growing radical (31). A schematic representation of cyclization, crosslinking, and multiple crosslinking reactions is shown in Figure 4.6. A similar behavior was observed during the swelling studies reported for poly(N-vinyl-2-pyrrolidone/itaconic acid) and poly(acrylamide/maleic acid) hydrogel systems (40).

ศูนย์วิทยทรัพยากร
จุฬาลงกรณ์มหาวิทยาลัย

Table 4.4 Number-average molar mass between crosslinks, (\bar{M}_c) and the crosslinking density, ($q \times 10^{-2}$) of the synthesized poly(AAm-co-CA)

N-MBA Concentration (% wt.)	2% mol CA		10% mol CA	
	\bar{M}_c	Crosslinking density (q)	\bar{M}_c	Crosslinking density (q)
0.5	898	8.01	1192	6.25
1.0	522	13.9	1000	7.49
1.5	450	16.2	976	7.71
2.0	405	18.1	945	8.01

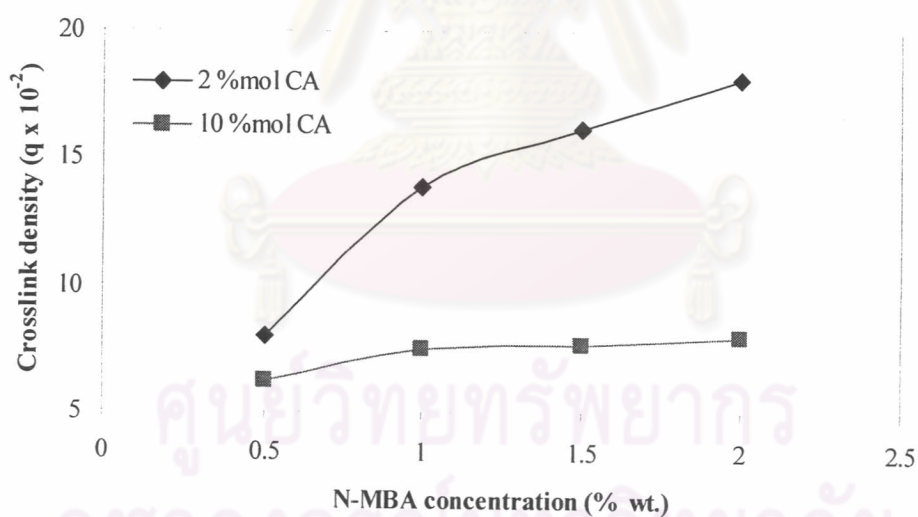


Figure 4.5 Effect of crosslinking agent concentration on the crosslinking density.

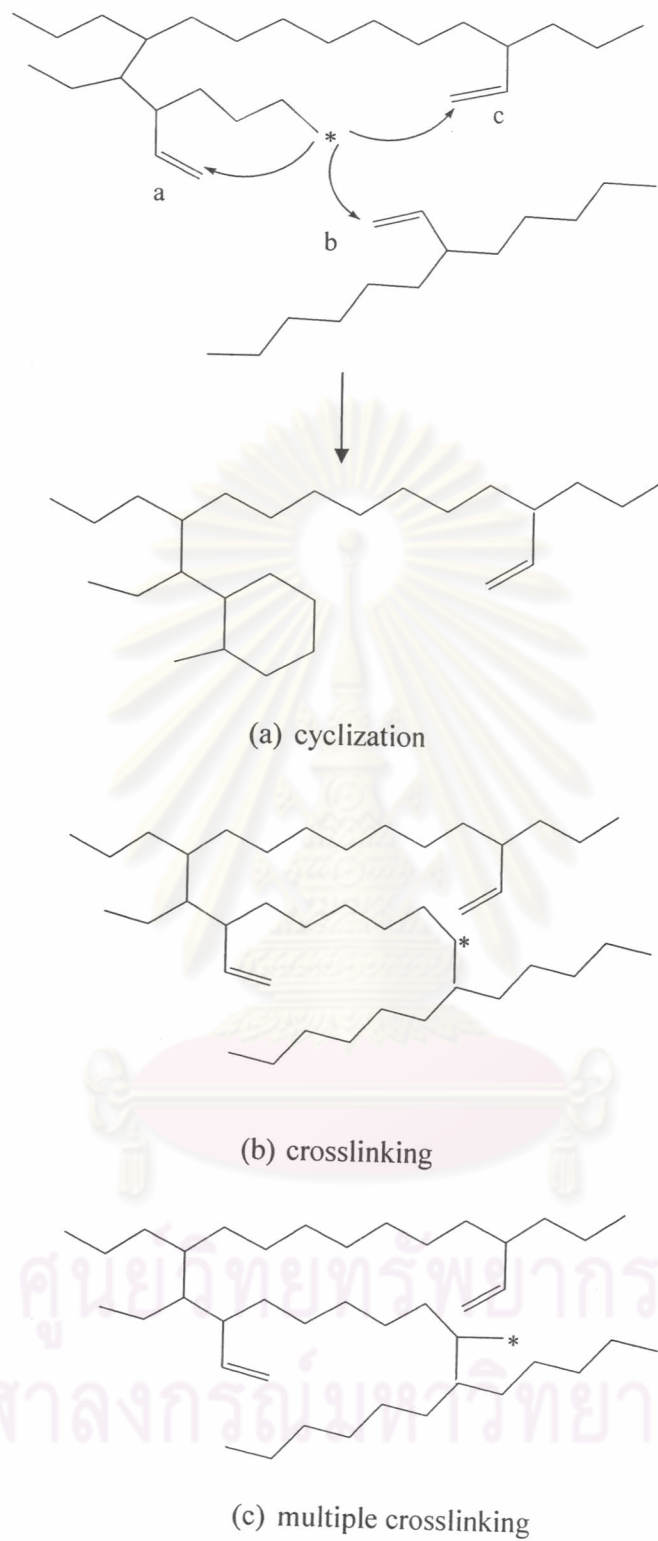


Figure 4.6 Schematic drawing of the reactions of cyclization (a), crosslinking (b), and multiple crosslinking (c) in the free-radical crosslinking copolymerization.

4.4 Effect of the Polymerization Temperature

The water absorbency of the copolymers synthesized by crosslinking polymerization at various temperatures is shown in Table 4.5 and Figure 4.7.

Table 4.5 Effect of the polymerization temperature on the water absorbency (Q) of the synthesized copolymer at 98/2 and 90/10 mole ratios of AAm/CA*

Temperature (°C)	Water absorbency (Q) g g ⁻¹	
	AAm/CA: 98/2	AAm/CA : 90/10
40	117±6	100±3
50	117±7	111±8
60	107±9	99±5
70	90±4	85±9

*Polymerization reactions were carried out at 1% APS, 2% TEMED, 1% N-MBA, 7% LF127, 28% NaHCO₃, 250 rpm and 30 min.

ศูนย์วิทยทรัพยากร
จุฬาลงกรณ์มหาวิทยาลัย

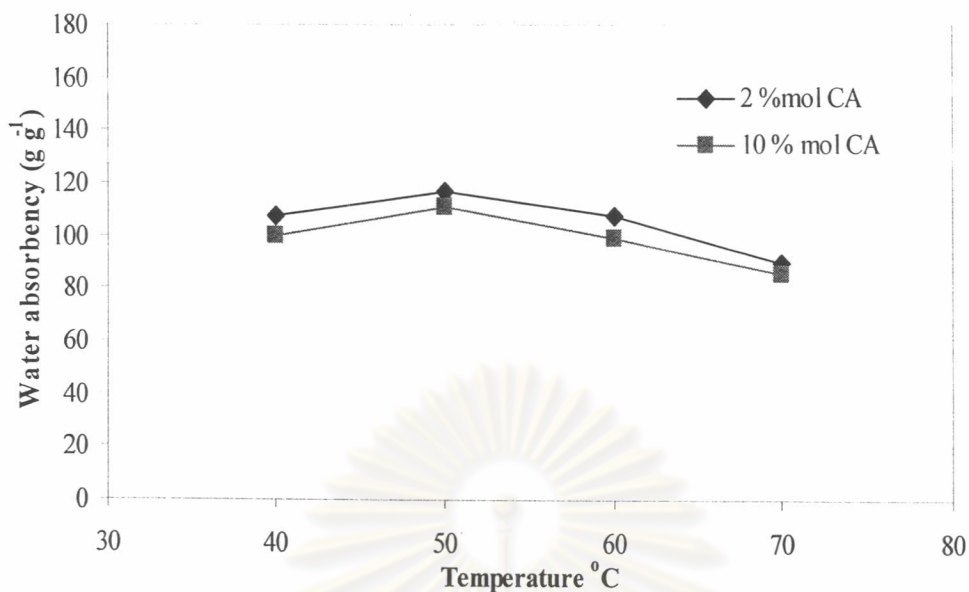


Figure 4.7 Effect of the polymerization temperature on the water absorbency (Q) of the synthesized copolymer at 1% APS, 2% TEMED, 1% N-MBA, 7% LF127, 28% NaHCO₃, 250 rpm and 30 min.

It is well known that in radical polymerization started by thermal decomposition of an initiator where transfer reactions are negligible. When reaction temperature is increased, the rate of polymerization is strongly enhanced and the molecular weight of the polymer is reduced because of increases of the rate termination and transfer reactions (41). The effect of polymerization temperature on the absorption capacity of the synthesized copolymer is shown in Figure 4.5. The water absorbency (Q) of the synthesized copolymer is decreased when the polymerization temperature is increased because an increase of polymerizing temperature decreases the molecular weight with increasing a large amount of short kinetic chains. These short chains reduce the water absorption capacity, which is

probably caused by changes in the copolymer composition with temperature due to change in the length of the polymer chains.

4.5 Effect of Agitation Rate

The water absorbency of the superabsorbent polymer, synthesized by 98/2 and 90/10 mole ratios of AAm/CA with 1% wt. APS, 2% wt. TEMED, 1% wt. N-MBA and various stirring rates, is shown in Table 4.6 and Figure 4.8.

Table 4.6 Effect of agitation rate on the water absorbency (Q) of the synthesized copolymer*

Agitation rate (rpm)	Water absorbency (Q) g g ⁻¹	
	AAm/CA: 98/2	AAm/CA : 90/10
150	89±1	78±7
200	106±2	97±2
250	111±0	113±0

*Polymerization reactions were carried out at 1% APS, 2% TEMED, 0.5% N-MBA, 7% LF127, 28% NaHCO₃, 50°C and 30 min.

ศูนย์วิทยทรัพยากร
จุฬาลงกรณ์มหาวิทยาลัย

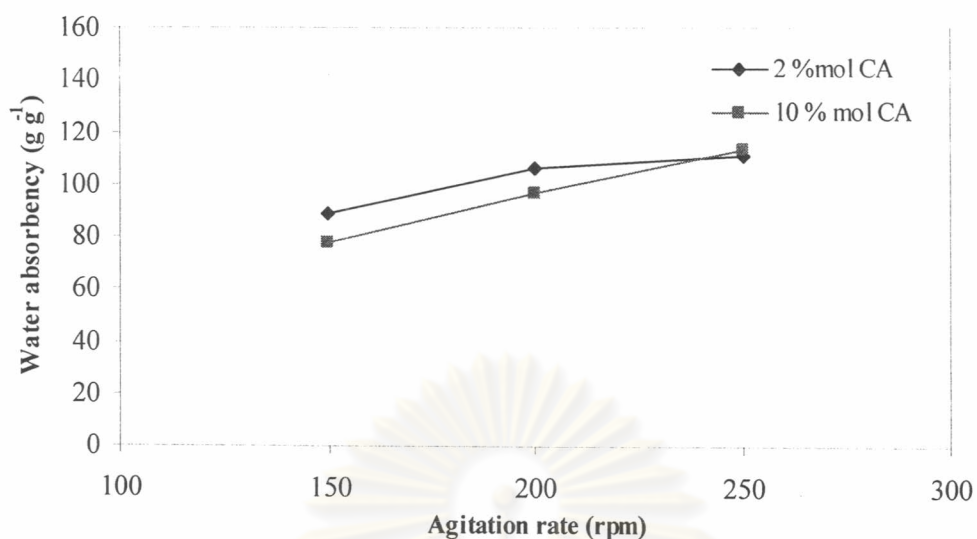


Figure 4.8 Effect of agitation rate on water absorbency (Q) of synthesized copolymer at 1% APS, 2% TEMED, 0.5% N-MBA, 7% LF127, 28% NaHCO₃, 50°C and 30 min.

In this system, the foam was produced from the reaction between sodium bicarbonate and crotonic acid. The agitation rate for sure affected the foam size and foam stability during the gel formation. The higher the agitation rate, the smaller the foam size and the less stable the foam. This leads to increasing water absorbency with increasing the agitation rate because the smaller size of the superabsorbent polymer can hold more interparticle water by the greater surface area.

4.6 Swelling Kinetics in Distilled Water

The swelling kinetics of the superabsorbent polymers prepared with the AAm-to-CA ratio of 98/2 were measured in distilled water as shown in Table 4.7 and Figure 4.9.

Table 4.7 Dependence of water absorbency on swelling time of the superabsorbent polymer*

Time (min)	Water absorbency (Q) g g^{-1}
5	56 \pm 5
10	126 \pm 4
20	142 \pm 7
30	182 \pm 2
40	196 \pm 3
50	200 \pm 6
60	202 \pm 4

*Polymerization reactions were carried out at 98/2 %mole AAm/CA, 1% APS, 2% TEMED, 0.5% N-MBA, 7% LF127, 28% NaHCO_3 , 50°C and 30 min.

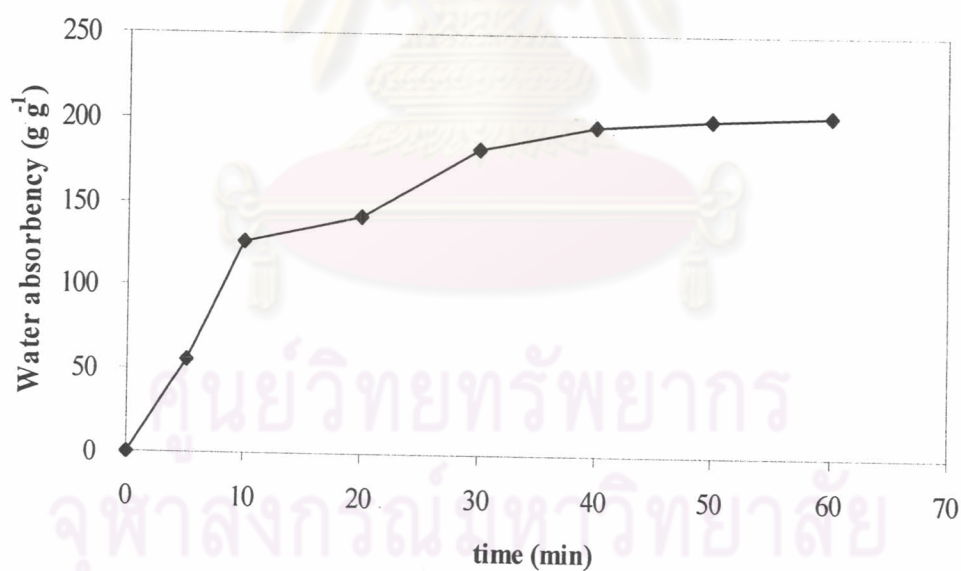


Figure 4.9 Dependence of water absorbency on swelling time of the superabsorbent polymer at 98/2 %mole AAm/CA, 1% APS, 2% TEMED, 0.5% N-MBA, 7% LF127, 28% NaHCO_3 , 50°C and 30 min.

The synthesized copolymer can absorb water up to 126 ± 4 g per g of the dry copolymer within 10 min. The dependence of swelling time on equilibrium swelling arises because the mass of liquid absorbed during the swelling rate measurement depends on the equilibrium swelling capacity of the polymer.

To examine the controlling mechanism of the swelling processes, several kinetic models are used to test experimental data. The large number and array of different chemical groups on the AAm/CA chains (e.g., amide, carbonyl, carboxyl or hydroxyl) imply that there are many types of polymer-solvent interactions. It is probable that any kinetic is likely to be applicable.

The main factor determining the swelling time of the dried porous superabsorbent polymer is the time needed for water to enter into the gel matrix and cover most of the surface of the pores. The effectiveness of the capillary action and wettability of pore surface are the two determinations for drawing water into the mass of the gel. The swelling kinetics of the superabsorbent polymer can be studied by application of a first-order kinetic expression based upon Fick's second law of diffusion (36), where C is concentration of the diffusing species, D is the diffusion coefficient of C , and r is the diffusion path length. For a spherical partical, the diffusion equation reduces to Equation 4.1 wherein the rate of swelling is first-order in the amount of swelling capacity remaining unswollen at any time, as given by Equations 4.2 and 4.3. The values of Q_{\max} and Q are the swelling capacities at equilibrium and at any time t . The first-order rate constant, k , depends on particle radius and on the diffusion coefficient (36), as shown in Figure 4.9.

$$\frac{\partial C}{\partial t} = \frac{1}{r} \frac{\partial}{\partial r} [rD \frac{\partial C}{\partial t}] \quad (4.1)$$

$$\frac{\partial Q}{\partial t} = k(Q_{\max} - Q) \quad (4.2)$$

$$Q(t) = Q_{\max} (1 - e^{-kt}) \quad (4.3)$$

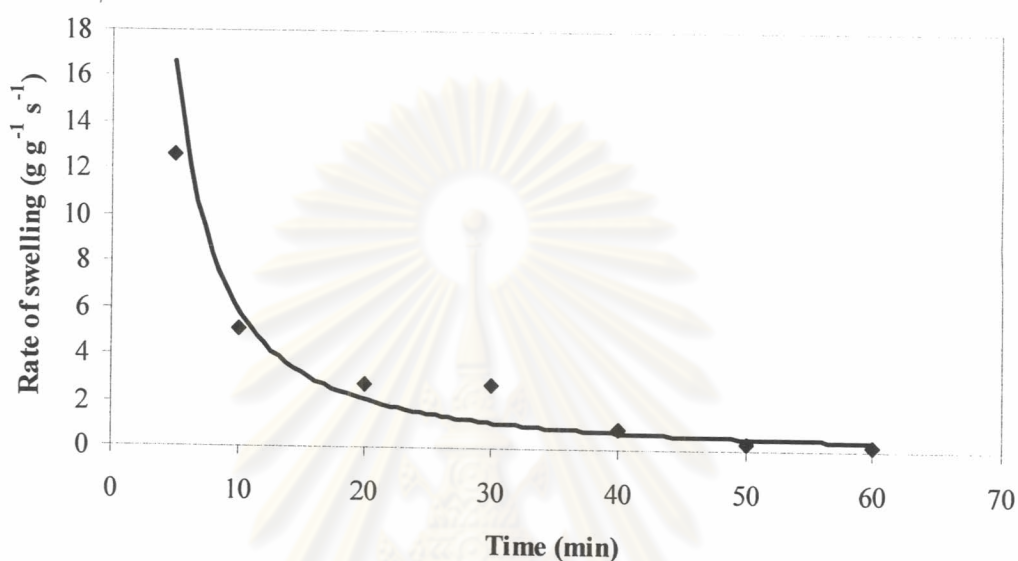


Figure 4.10 Swelling kinetics of the synthesized copolymer.

In this model of the dynamic swelling process, the structure of the polymer and the system affect the maximum swelling capacity Q_{\max} . In practical applications, not only a higher swelling absorption capacity, but also a higher swelling absorption rate is required for the superabsorbent polymer. The synthesized copolymer is also characterized by its rapid swelling kinetics as presented in Figure 4.10.

From the plot of Q_{\max} vs time in Figure 4.9, one gets a slope of the swelling kinetics of $6 \text{ g g}^{-1} \text{ s}^{-1}$. One can also calculate the rate constant of swelling (k) from the first-order kinetics at any time, t , (Equation 4.3). The k value depends on the

diffusion coefficient and the particle radius. For the rate of swelling, Equation 4.2 is applied to each absorption time. We found that the rate of swelling decreased with increasing swelling time. The swelling rate became stable or constant within 20 min, with a swelling rate of $2.8 \text{ g g}^{-1} \text{ s}^{-1}$. The faster swelling was then accompanied by a higher degree of swelling.

4.7 Characterization

4.7.1 FT-IR Spectra of the Synthesized Copolymers

The functional groups of the synthesized copolymer were investigated by Fourier Transform Infrared Spectroscopy (FTIR). The spectra are shown in Figures 4.11-4.13 and assignment in Table 4.8.

From the FTIR spectra, we found that the FTIR spectrum of synthesized copolymers confirms the existence of the carbonyl and carboxamide functionalities.

Table 4.8 Assignments for the FTIR spectrum of the synthesized poly(acrylamide)

Wave number (cm^{-1})	Assignment
3459, strong	N-H stretching
2921, sharp and strong	C-H stretching CH_3 and CH_2 (aliphatic)
1653, strong	C=O stretching of $-\text{CONH}_2$
1404, weak	C-H asymmetric bending
1314, weak	C-N aliphatic stretching

Table 4.9 Assignments for the FTIR spectrum of the synthesized poly[acrylamide-*co*-crotonic acid)]

Wave number (cm ⁻¹)	Assignment
3427, strong	O-H stretching
2925, sharp and strong	C-H stretching CH ₃ and CH ₂ (aliphatic)
1664, strong	C=O stretching of -CONH ₂
1450, weak	C-H asymmetric bending
1411, weak	C=O symmetric stretching for carboxylate ion
1318, weak	C-N aliphatic stretching

4.7.2 Surface Morphology of the Synthesized Copolymers

The synthesized copolymers were investigated by SEM technique to observe the surface appearance. The electron micrographs of the crosslinked copolymers are shown in Figures 4.14 to 4.16. Polymer particles from the foamed solution polymerization were irregular in shape. The SEM micrograph of the synthesised polyacrylamide in Figure 4.14 have fine network and smooth surface, the water absorbency of the synthesised polyacrylamide was lower than that of the poly(AAm-*co*-CA). The SEM micrograph of the synthesized poly(AAm-*co*-CA) with 2 percent mole of CA gave high water absorbency as shown in Figure 4.15. However, the SEM micrograph of the synthesised poly(AAm-*co*-CA) with CA percent mole of 30 in Figure 4.16 shows more microporous structure with a less flexible, cellular structure.

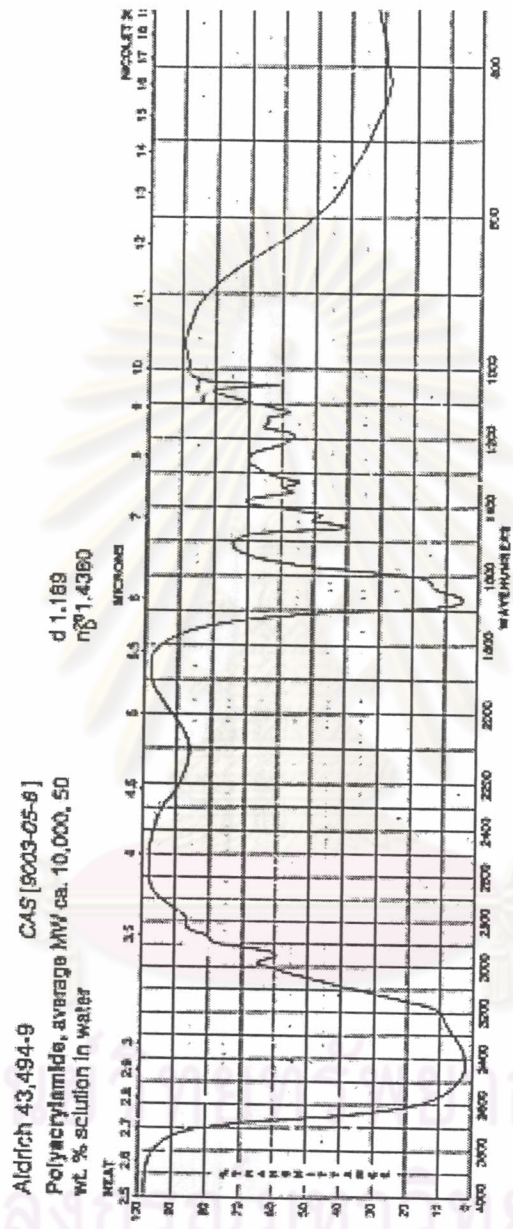


Figure 4.11 FT-IR spectrum of poly(acrylamide).

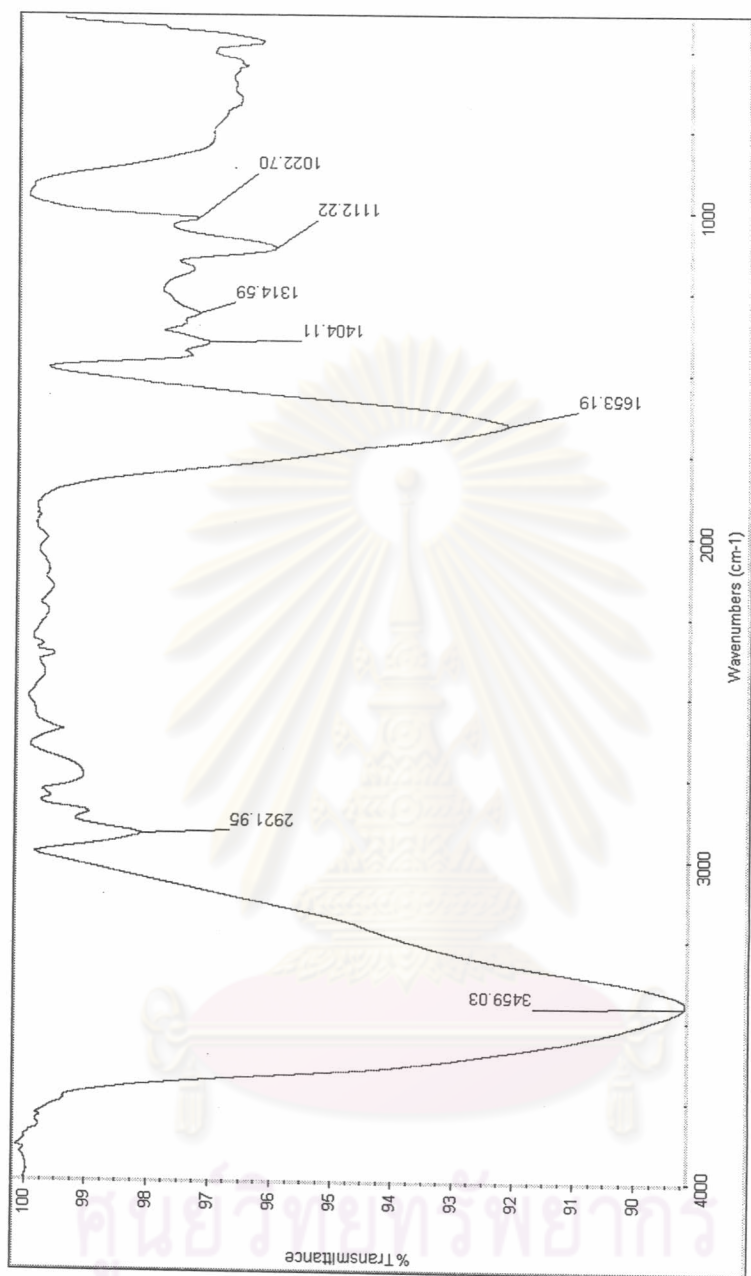


FIGURE 4.12 FT-IR spectrum of synthesized poly(acrylamide).

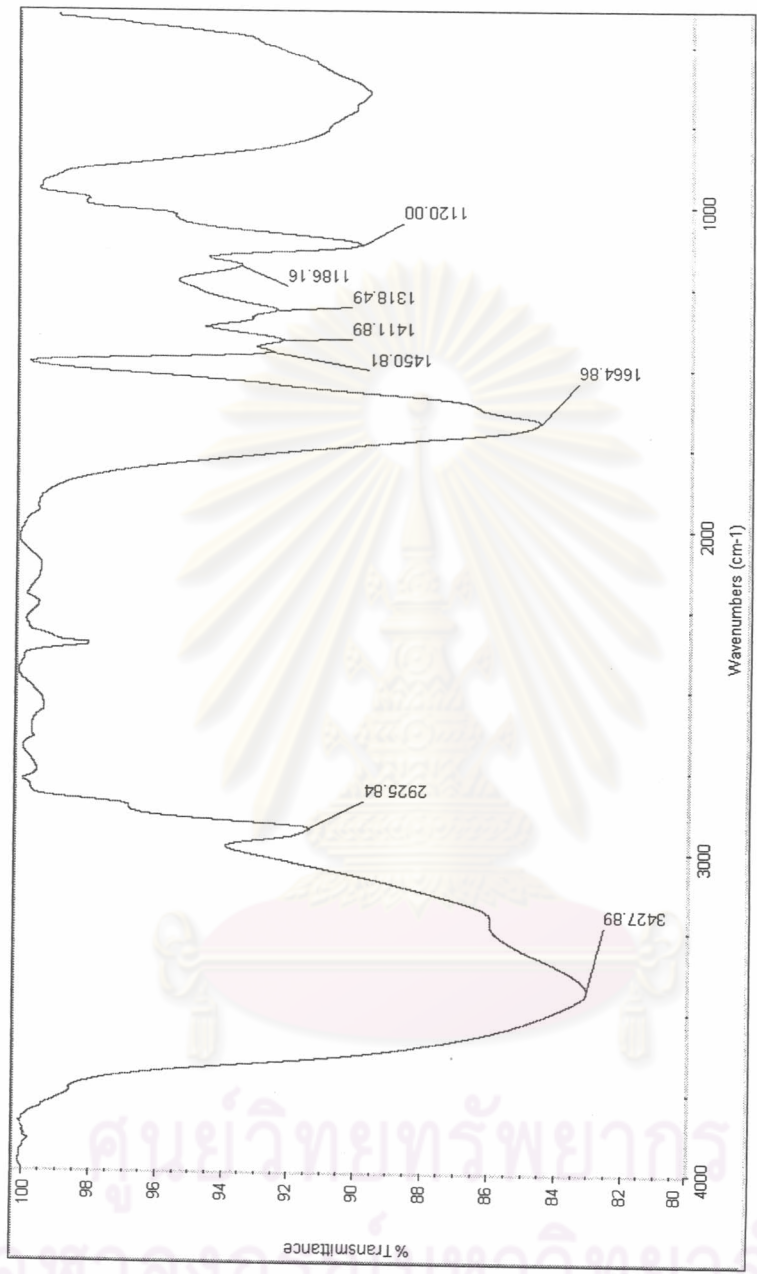


Figure 4.13 FT-IR spectrum of synthesized poly[acrylamide-co-(crotonic acid)].

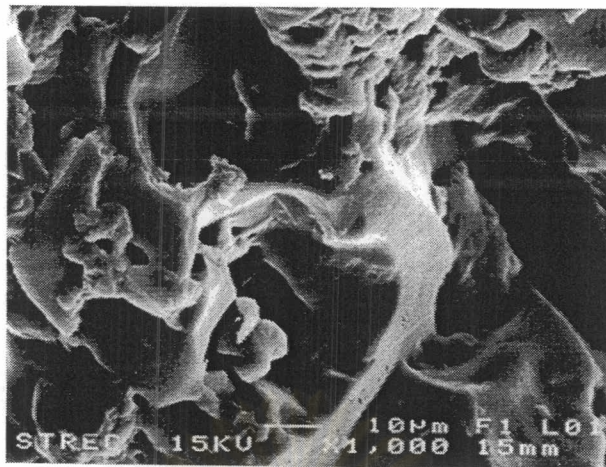


Figure 4.14 SEM micrograph of polyacrylamide (Water absorbency = $54 \pm 4 \text{ g g}^{-1}$).

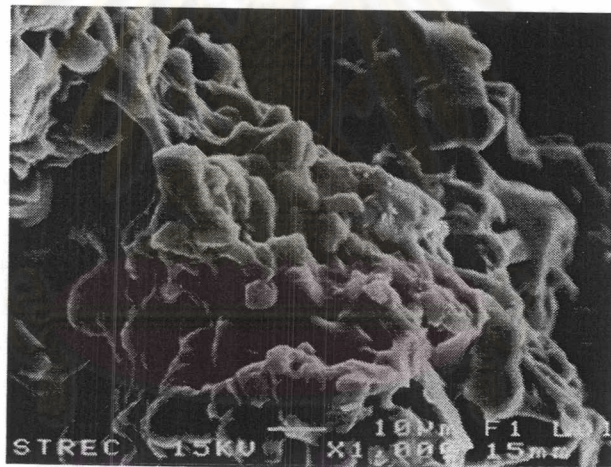


Figure 4.15 SEM micrograph of poly(AAm-co-CA) with CA percent mole of 2 (Water absorbency = 211 g g^{-1}).

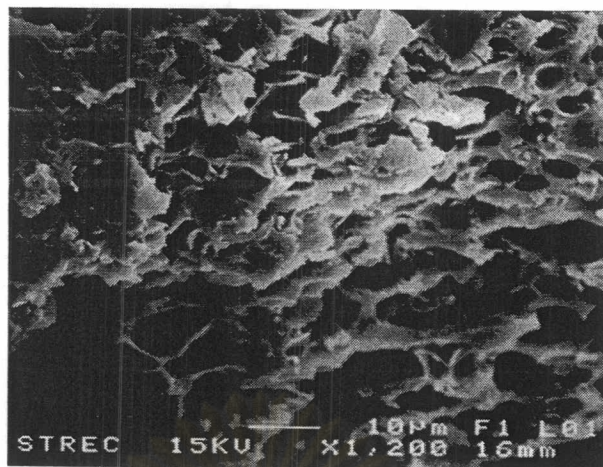


Figure 4.16 SEM micrograph of poly(AAm-co-CA) with CA percent mole of 30 (Water absorbency = 130 g g^{-1}).

4.7.3 Investigation of the Redox Reaction of Monomer, Co-monomer, Initiator, and Crosslinking Agent and Kinetic by Cyclic Voltammetry

In order to understand interaction of monomer and co-monomer, cyclic voltammetry, the electrochemical technique is the one that is effective and versatile available for the mechanistic study of redox systems. This technique can be used for studying the relation between the current and the potential by rapidly scanning. In this research, voltammetric behaviors of monomer, co-monomer, initiator and crosslinking agent were investigated by cyclic voltammetry (CV) using a glassy carbon as a working electrode, Ag/AgCl (sat. KCl) as a reference electrode, platinum wire as an auxiliary electrode and 0.1 M KCl as supporting electrolyte.

4.7.3.1 Study redox reaction of monomer, co-monomer, initiator and crosslinking agent

The cyclic voltammograms of supporting electrolyte, monomer, co-monomer, initiator and crosslinking agent are presented in Figures 4.17 to 4.21. The cyclic voltammograms characterized several important parameters to confirm the redox reactions. The reversible process exhibited the ΔE_p value about 0.059 V and the ratio of i_{pa} to i_{pc} is unity. The quasi-reversible displayed the ΔE_p value more than 0.059 V. The irreversible process, only oxidation or reduction peak is obtained. The individual peak was reduced in size and widely separated. The background of 0.1 M KCl is shown in Figure 4.17.

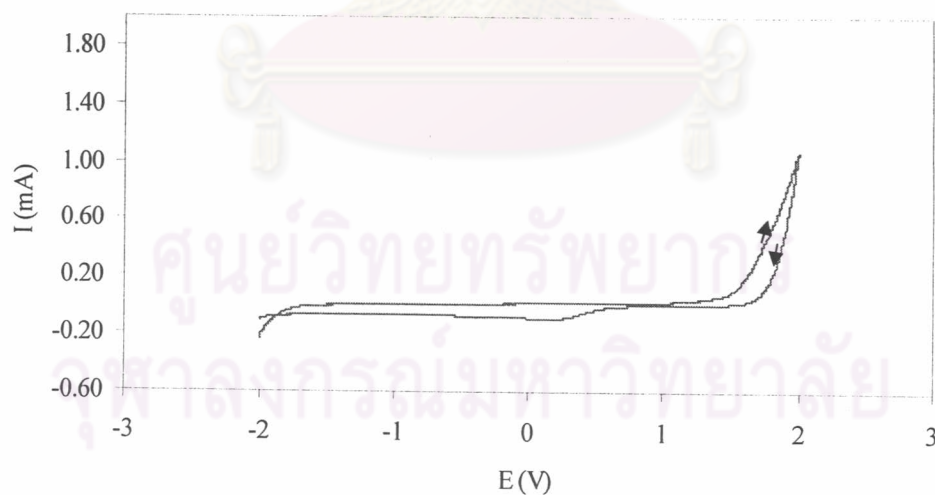


Figure 4.17 Cyclic voltammogram of 0.1 M KCl using a glassy carbon as a working electrode, the scan rate is 50 mV/s.

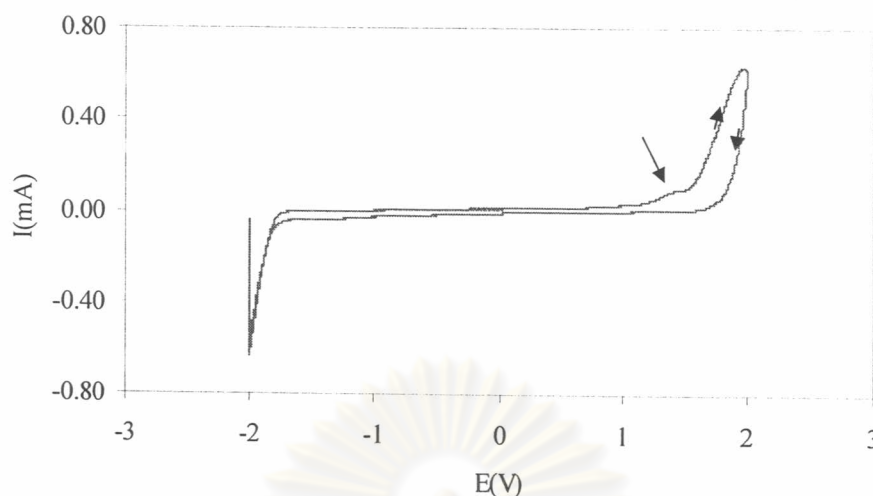


Figure 4.18 Cyclic voltammogram of AAm in 0.1 M KCl using a glassy carbon as a working electrode, the scan rate is 50 mV/s.

The voltammogram of AAm in a supporting electrolyte (0.1 M KCl) is shown in Figure 4.18. When increasing voltage, the oxidation of AAm starts at about 1.1 V until zero of the sample concentration surrounding working electrode is reached . The Anodic wave at $E_{pa} = 1.5$ V shows $I_{pa} = 0.98$ mA. In the reverse cathodic direction, cathodic wave was not appeared. The voltammogram indicates the irreversible nature of AAm. Thus AAm should be electron donor in the reaction.

ศูนย์วิทยทรัพยากร
จุฬาลงกรณ์มหาวิทยาลัย

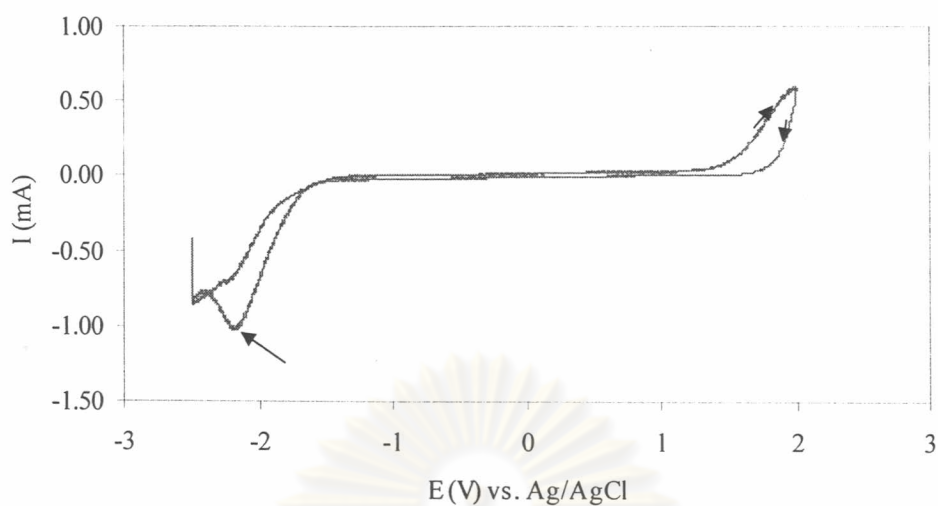


Figure 4.19 Cyclic voltammogram of CA in 0.1 M KCl using a glassy carbon as a working electrode, the scan rate is 50 mV/s.

The voltammogram of CA in a supporting electrolyte (0.1 M KCl) is shown in Figure 4.19. With decreasing the voltage to more negative potential the started reduction of CA at about -1.7 V is found. The resulting cathodic wave at $E_{pc} = -2.2$ V shows $I_{pc} = 1.0$ mA. However, the voltammogram indicates the irreversible nature of CA. Thus CA should be electron acceptor in the reaction.

ศูนย์วิทยทรัพยากร
จุฬาลงกรณ์มหาวิทยาลัย

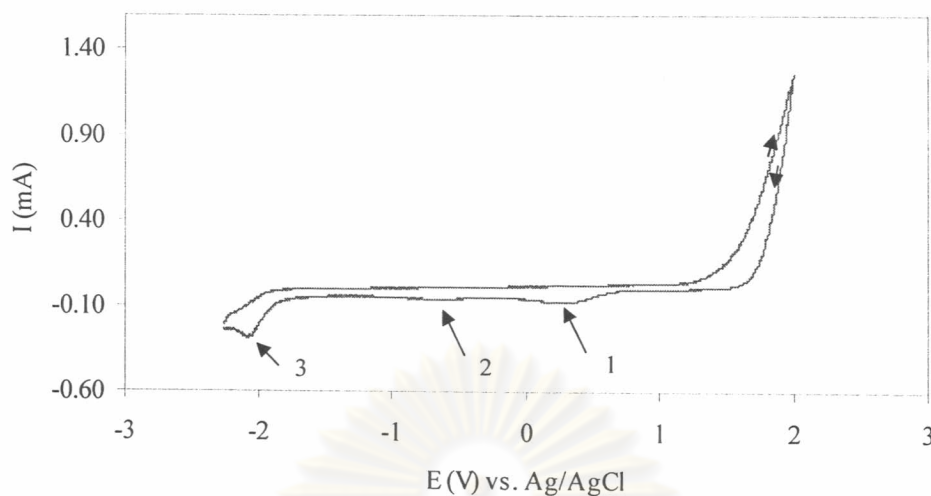


Figure 4.20 Cyclic voltammogram of N-MBA in 0.1 M KCl using a glassy carbon as a working electrode, the scan rate is 50 mV/s.

The voltammogram of N-MBA in a supporting electrolyte (0.1 M KCl) is shown in Figure 4.20. N-MBA shows three reduction peaks (cathodic peaks) when decreasing the voltage to more negative potential. The first cathodic wave at $E_{pc} = 0.50$ V shows $I_{pc} = 0.10$ mA, the second cathodic wave at $E_{pc} = -0.50$ V shows $I_{pc} = 0.1$ mA., and the third cathodic wave at $E_{pc} = -2.0$ V shows $I_{pc} = 0.27$ mA.

ศูนย์วิทยทรัพยากร
จุฬาลงกรณ์มหาวิทยาลัย

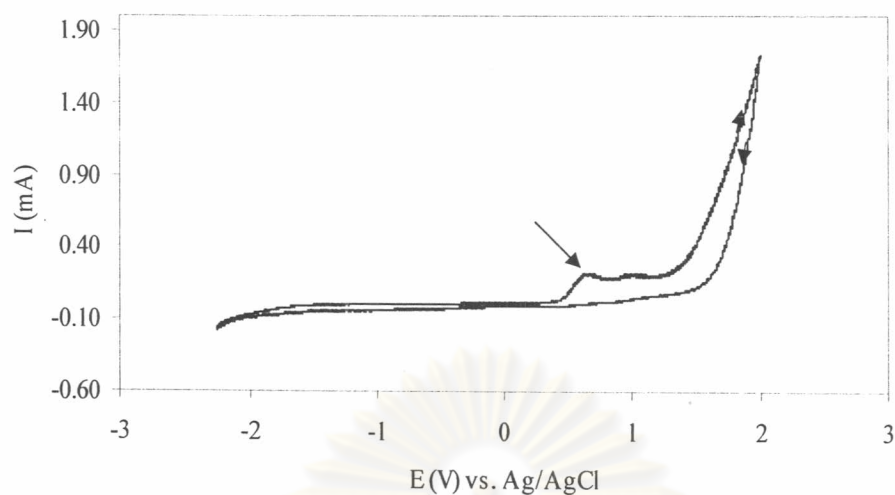


Figure 4.21 Cyclic voltammogram of APS and TEMED in 0.1 M KCl using a glassy carbon as a working electrode, the scan rate is 50 mV/s.

The voltammogram of APS and TEMED in a supporting electrolyte (0.1 M KCl) is shown in Figure 4.21. When increasing voltage, the oxidation of APS and TEMED starts at about 0.5 V, until zero of the sample concentration surrounding working electrode is reached. The Anodic wave at $E_{pa} = 0.65$ V shows $I_{pa} = 0.21$ mA. In the reverse cathodic direction, cathodic wave was not appeared.

The summarized parameters of importance of cyclic voltammograms from electrochemical behavior of the monomer, co-monomer, initiator and crosslinking agent are shown in Table 4.10.

Table 4.10 Important parameters of cyclic voltammograms from electrochemical behavior of monomer, co-monomer, initiator and crosslinking agent.

Sample	E_{pa} (V)	i_{pa} (mA)	E_{pc} (V)	i_{pc} (mA)
AAm	1.5	0.98	-	-
CA	-	-	-2.2	1.0
N-MBA	-	-	0.5	0.1
	-	-	-0.5	0.1
	-	-	-2.0	0.27
APS+TEMED	0.65	0.21	-	-

ศูนย์วิทยทรัพยากร
จุฬาลงกรณ์มหาวิทยาลัย

4.7.3.2 Kinetic Study of Polymerization

The kinetic study of reaction was investigated for understanding mechanism of gelation by cyclic voltammetry. The kinetic voltammogram results are presented in Figures 4.22 to 4.28.

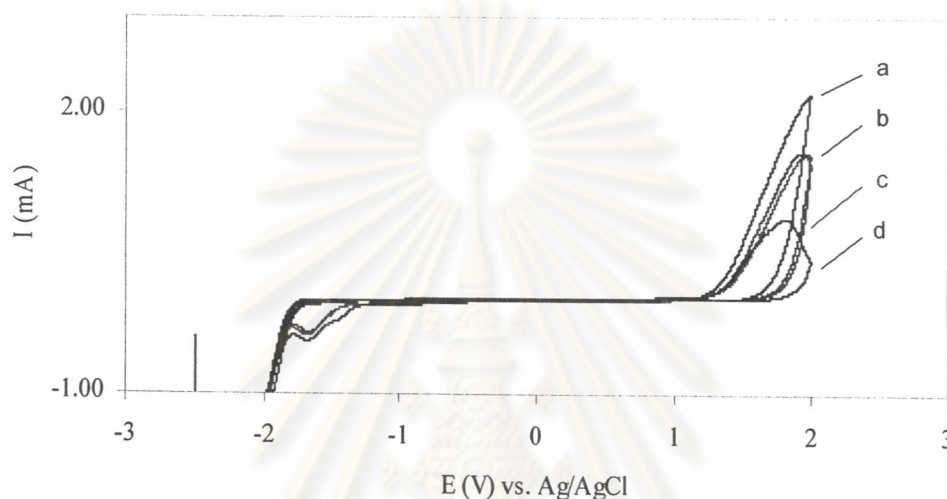


Figure 4.22 Cyclic voltammograms of a: AAm, b: AAm+CA, c: AAm+CA+N-MBA, d: AAm+CA+N-MBA+APS in 0.1 M KCl using a glassy carbon as a working electrode, the scan rate is 50 mV/s

There are some difference in the cyclic voltammograms of AAm, AAm+CA, AAm+CA+N-MBA, and AAm+CA+N-MBA+APS in the oxidation direction as well as in the reduction direction as seen in the Figure 4.22. After adding APS, cycling voltammogram gave a new oxidation peak at $E_{pa} = 1.8$ V and the same reduction peak at $E_{pc} = -2.3$ V. The important parameters of cyclic voltammograms from electrochemical behavior after adding monomer, co-monomer, initiator and crosslinking agent in a sequential addition is shown in Table 4.11.

Table 4.11 Important parameters of cyclic voltammograms from electrochemical behavior after adding monomer, co-monomer, initiator and crosslinking agent in a sequential addition.

Sample	E_{pa} (V)	i_{pa} (mA)	E_{pc} (V)	i_{pc} (mA)
AAm	1.98	2.07	-	-
AAm+CA	1.98	1.49	-1.70	0.31
AAm+CA+ N-MBA	1.98	1.49	-1.70	0.31
AAm+CA+ N-MBA+APS+ TEMED	1.80	0.83	-1.70	0.40

ศูนย์วิทยทรัพยากร
จุฬาลงกรณ์มหาวิทยาลัย

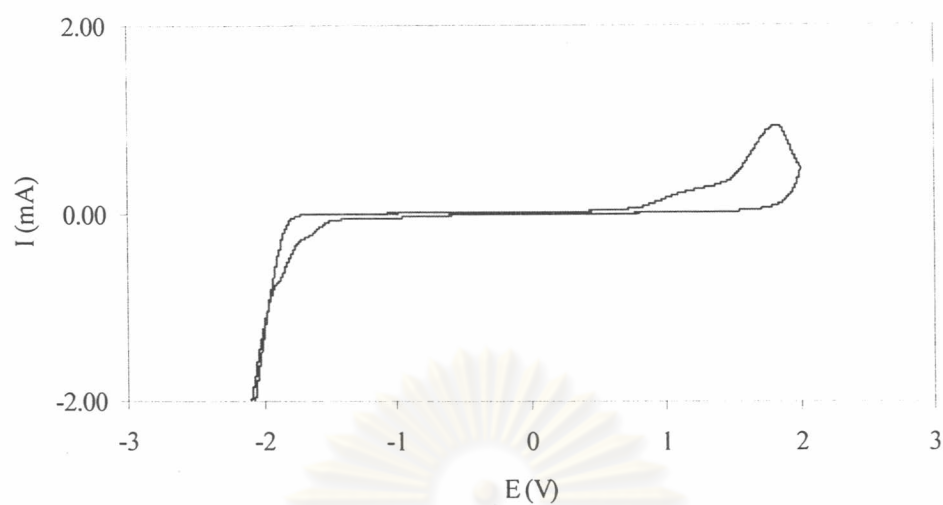


Figure 4.23 Cyclic voltammogram after adding TEMED at 7.09 min as in the same conditions of Figure 4.22.

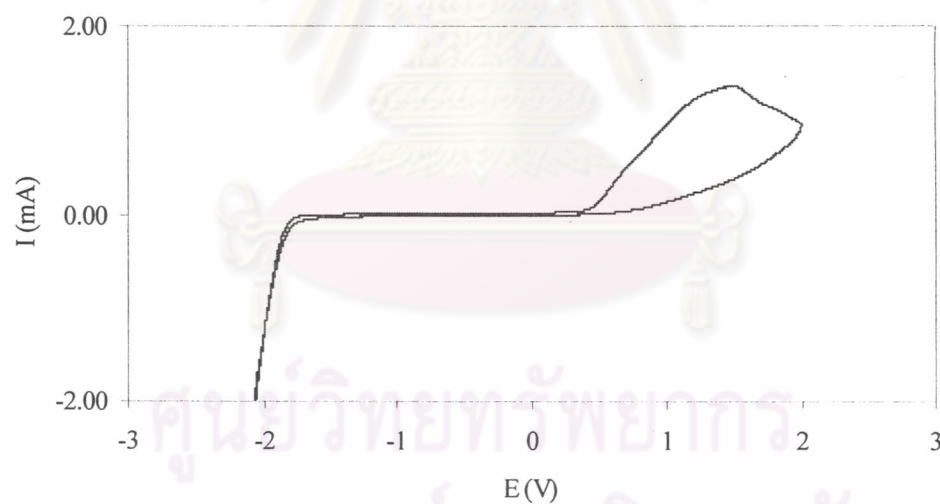


Figure 4.24 Cyclic voltammogram after adding TEMED at 11.07 min as in the same conditions of Figure 4.22.

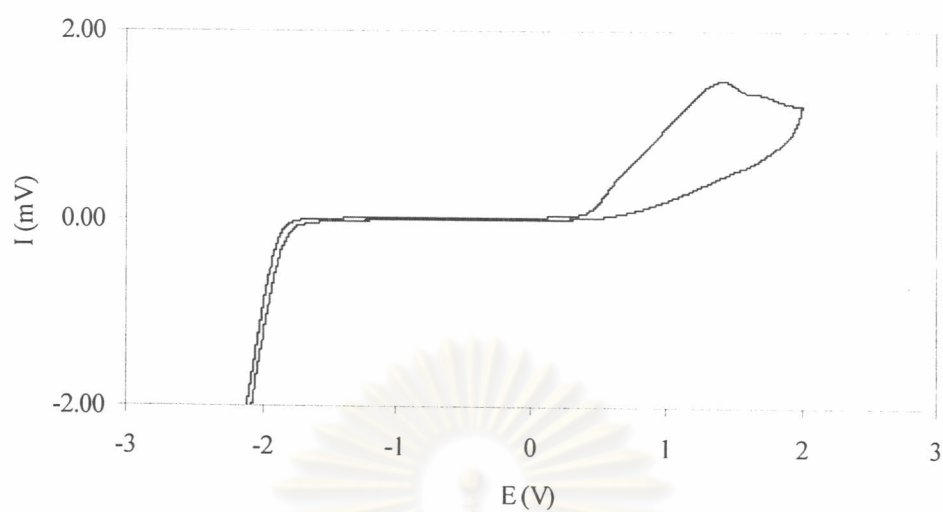


Figure 4.25 Cyclic voltammogram after adding TEMED at 15.03 min as in the same conditions of Figure 4.22.

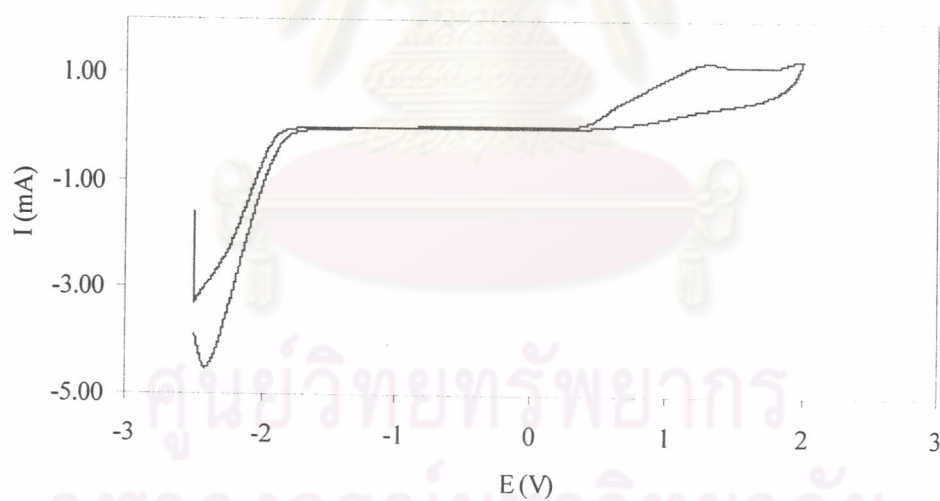


Figure 4.26 Cyclic voltammogram after adding TEMED at 19.26 min as in the same conditions of Figure 4.22.

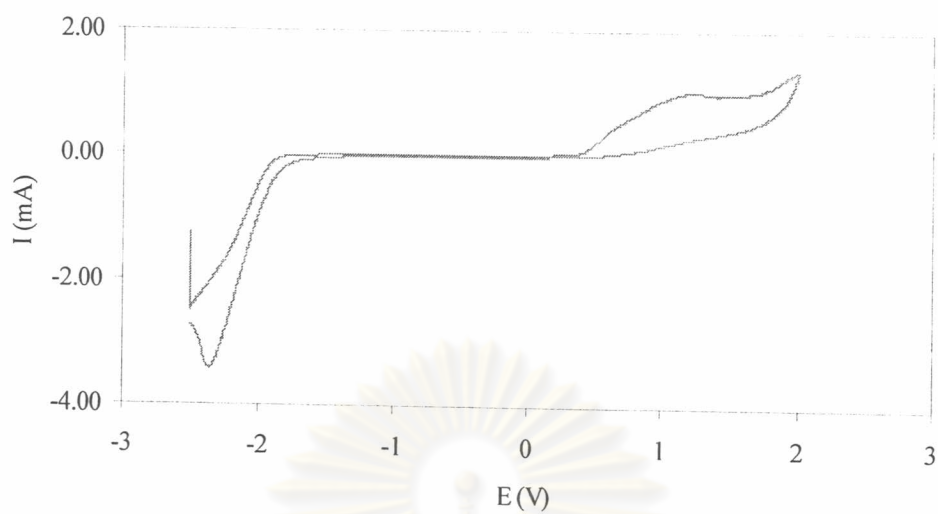


Figure 4.27 Cyclic voltammogram after adding TEMED at 23.20 min as in the same conditions of Figure 4.22.

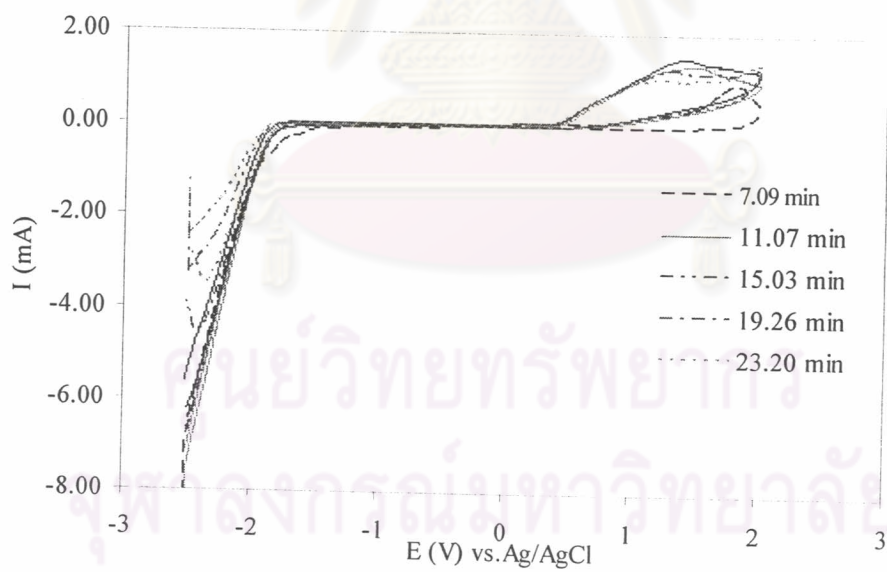


Figure 4.28 Cyclic voltammogram after adding TEMED as in the same conditions of Figure 4.22.

As seen in Figures 4.23-4.28, upon taking multiple cyclings of the solution, a new peak develops at a lower potential after adding TEMED in the oxidation direction. There are some transfer electrons in the polymerization reaction. Table 4.12 shows several important parameters taking place in the reaction: the cathodic (E_{pc}) and anodic (E_{pa}) peak potentials, the cathodic (i_{pc}) and anodic (i_{pa}) peak currents. The first cycle after the addition of TEMED to the reaction at 7.09 min is given in Figure 4.23. The oxidation begins at 1.8 V. After repeating the cycle at 11.07 min and 15.03 min, the cyclic voltammogram of Figure 4.24 and Figure 4.25 are obtained. The anodic current increase from 0.8 to 1.6 mA (in Figure 4.24) then drops from 1.6 to 1.4 mA (in Figure 4.25). Furthermore voltammogram taking after 19.26 min cycling gave a new reduction peak at $E_{pc} = 2.3$ V. A smaller shift of E_{pc} of reduction peak was also seen after taking 23.20 min cycling. The anodic and cathodic current drops from 1.2 to 1.0 mA and 4.6 to 3.6 mA (in Figure 4.27) due to increasing viscosity and the resulting decreasing in ion mobility as the medium evolves from solution to gel state.

Table 4.12 Important parameters of cyclic voltammograms from kinetics study of the synthesized hydrogels.

Time (min)	E_{pa} (V)	i_{pa} (mA)	E_{pc} (V)	i_{pc} (mA)
7.09	1.8	0.8	-	-
11.07	1.6	1.6	-	-
15.03	1.5	1.4	-	-
19.26	1.2	1.2	2.3	4.6
23.20	1.1	1.0	2.4	3.6

To characterize the reaction products at 7.37, 13.40, and 21.53 min., FT-IR was used for proving the functional groups of reaction products as seen in Table 4.13.

Table 4.13 Assignments for the FTIR spectrum of the synthesized poly[acrylamide-co-crotonic acid)] from electrochemical cell at 7.37, 13.40, and 21.53 min.

Wave number (cm ⁻¹)	Assignment
3431, strong	O-H stretching
2929, sharp and strong	C-H stretching CH ₃ and CH ₂ (aliphatic)
1664, strong	C=O stretching of -CONH ₂
1446, weak	C-H asymmetric bending
1415, weak	C=O symmetric stretching for carboxylate ion
1318, weak	C-N aliphatic stretching

ศูนย์วิทยทรัพยากร
จุฬาลงกรณ์มหาวิทยาลัย

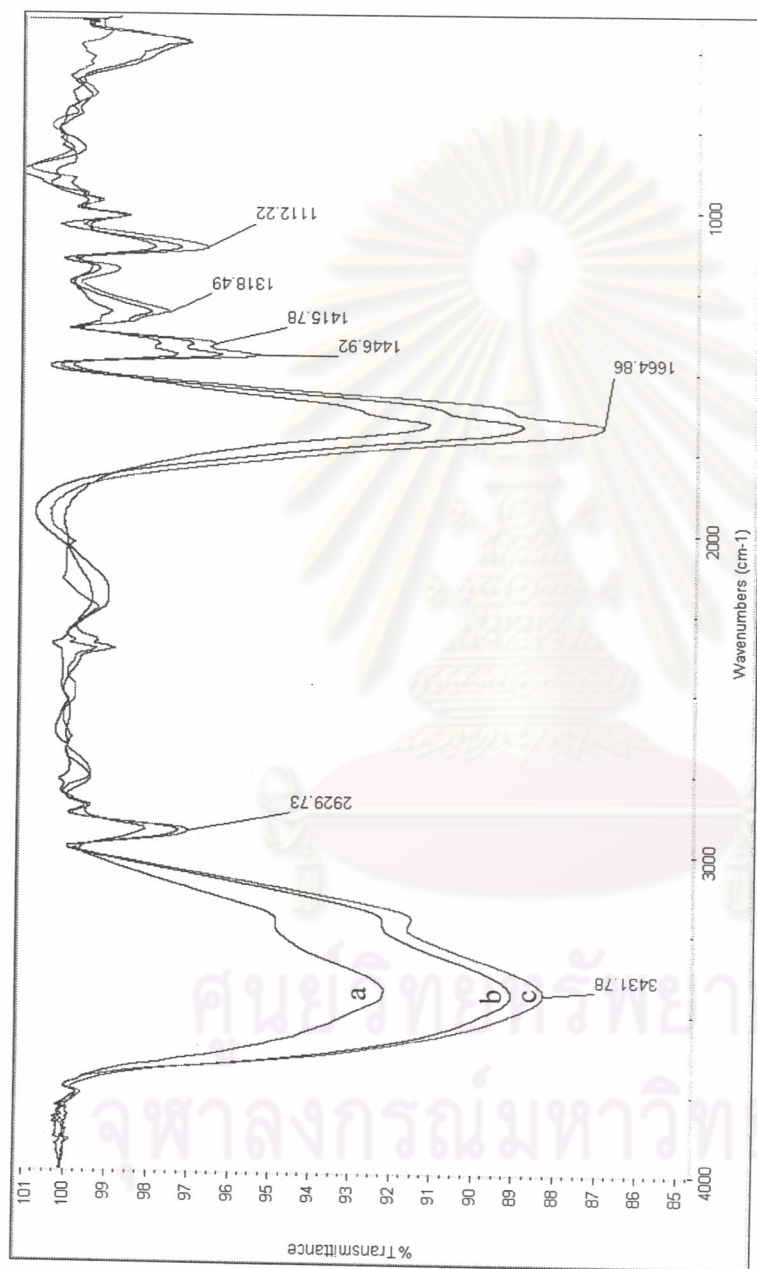


Figure 4.29 FT-IR spectrum of synthesized poly[acrylamide-co-(crotonic acid)] from electrochemical cell at any time a) 7.37 min, b) 13.40 min, and c) 21.53 min.

4.8 Application of Superabsorbent Copolymer in Removing Dye Pollutants

4.8.1 Effect of Structure of Dye

To observe the adsorption of some dyes, polyacrylamide and poly(AAm/CA) hydrogels were placed in aqueous solutions of cationic dyes, basic blue 41(BB-41) and the aqueous solutions of anionic dyes, direct blue 85 and they were allowed to equilibrate for 1 day in 20 mg dye⁻¹ of aqueous solution. The chemical structure of BB-41 dye is shown in Figure 4.30. At the end of the equilibrate time, comparison between the two dye solutions can be seen in Figure 4.31. The poly(AAm/CA) hydrogel in the aqueous of solution of BB-41 gave high adsorption with increasing the CA content whereas poly(AAm/CA) hydrogel could not adsorb the anionic dyes (Direct blue 85). Since ionizable groups (the carboxylate anion) of the polymer increased in the presence of crotonic acid beside the acrylamide group. Therefore interactions (acid-base and electrostatic) between the cationic groups of cationic dyes and carboxylate groups of the P(AAm/CA) superabsorbent gel increases with increasing cationic groups in polymer chain. On the other hand, there is an anionic repulsion between the anionic groups of anionic dyes and the carboxylate group of CA in the hydrogels and therefore no interaction between the anionic dyes and poly(AAm/CA) hydrogels can occur to adsorb the anionic dyes.

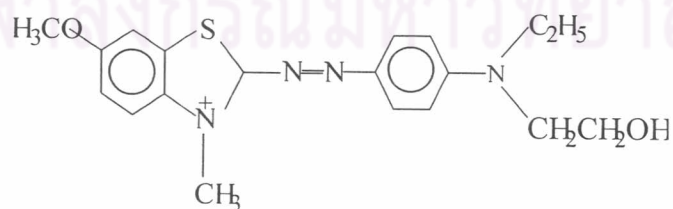


Figure 4.30 The chemical structure of BB-41 dye (CI 11105).

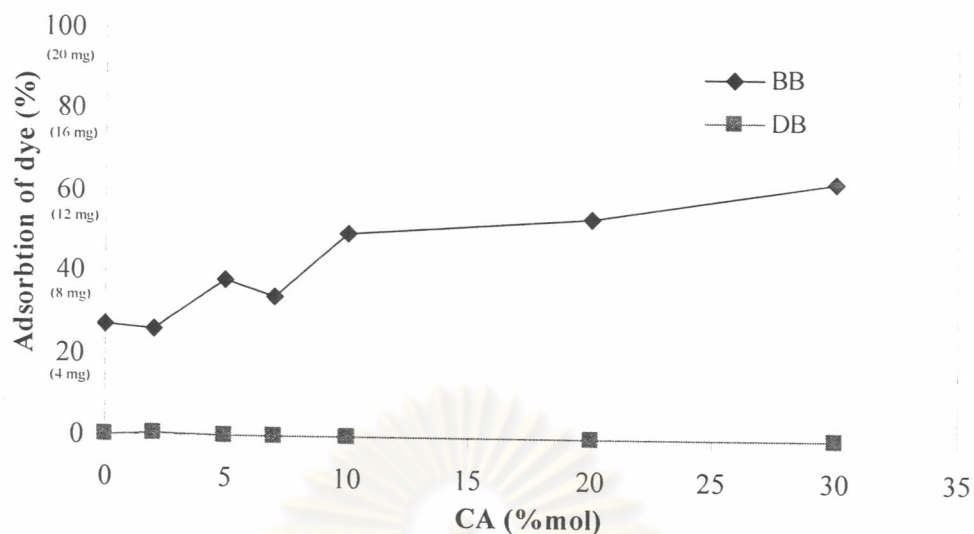


Figure 4.31 Efficiency of hydrogels on different structure of dye.

The other type of interaction between the anionic superabsorbent polymer and cationic dyes can be the hydrophobic interaction. Hydrophobic interaction in the present case involves the aromatic rings and the methyl groups on the gel. Therefore the polyacrylamide gel could adsorb the dye about 25% of initial dye concentration as seen in Figure 4.31. Electrostatic interactions between the dye molecule and the hydrogel is the dominant attribute to decolor the dye as shown in Figure 4.32.

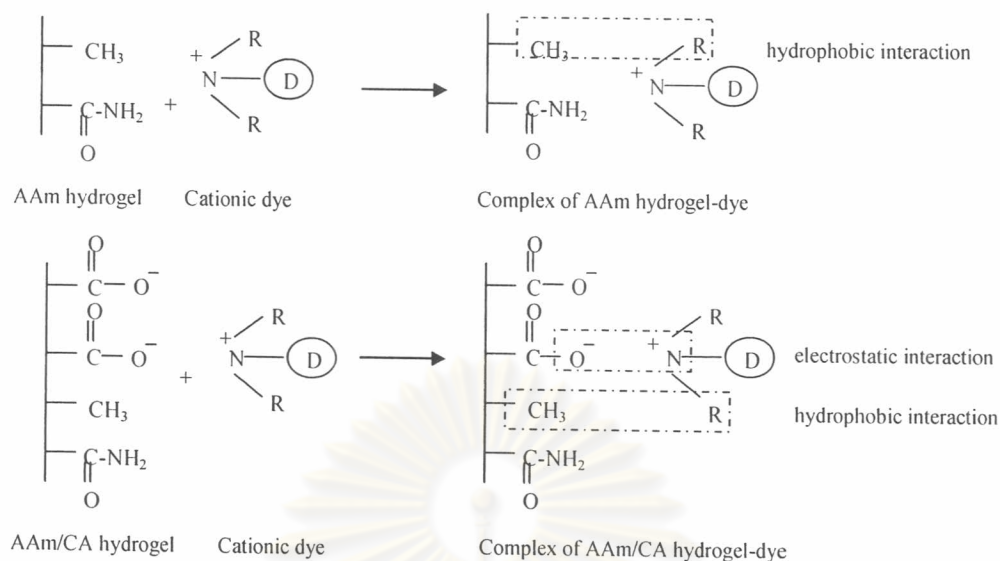


Figure 4.32 Possible complexation reaction between AAm/CA hydrogel and dye molecule.

4.8.2 Effects of Crotonic Acid Content and pH of the Dye Solution on Swelling Time and Dye Adsorption

The influences of the crotonic acid content in the superabsorbent polymer and the pH of the dye solution on water swelling and the dye adsorption (BB-41) of poly(AAm/CA) hydrogels are presented in Figures 4.33-4.34.

ศูนย์วิทยทรัพยากร
จุฬาลงกรณ์มหาวิทยาลัย

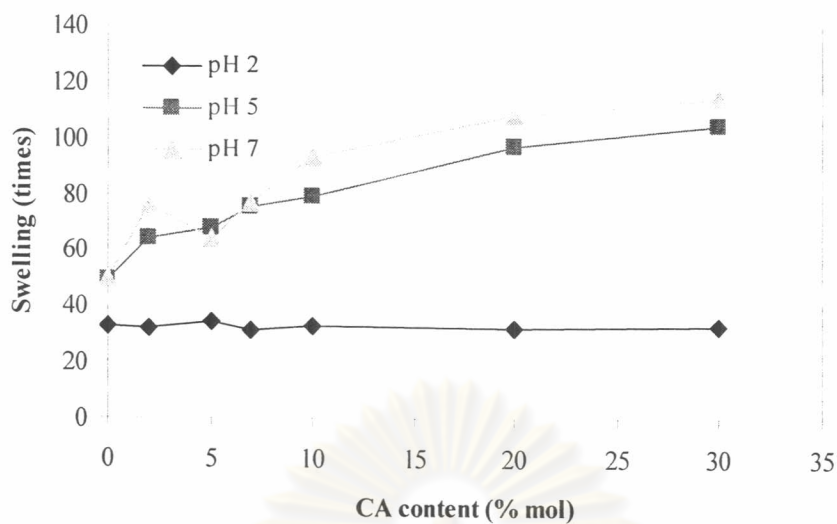


Figure 4.33 Effect of crotonic acid content at different pHs on swelling of the copolymers.

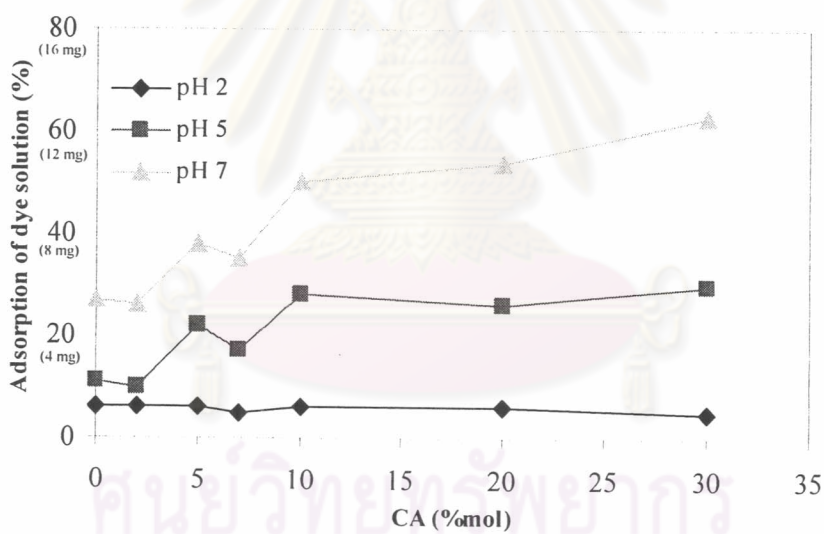


Figure 4.34 Effect of poly(AAm/CA) hydrogels on removing cationic dye solution at different pHs.

In the Figure 4.33, the effect of crotonic acid content on the swelling at pH 2, dye solution of is constant regardless of the highest constant of 30 % mole CA. At the high pH , the swelling of the poly(AAm/CA) hydrogels was observed. An increase in pH from 2 to 7 caused a significant increase in swelling of the hydrogels with a higher crotonic acid content. The equilibrium swelling for poly(AAm/CA) hydrogels at different compositions and the efficiency of poly(AAm/CA) on removing the cationic dye solution is at maximum at pH 7. The swelling of superabsorbent polymer is directly proportional to the degree of ionization of the polymer. Consistent results with the polyelectrolyte system, especially for the high crotonic acid content of hydrogels, a sudden increase was observed at pH 5 and pH 7 due to the complete dissociation of the acidic groups of CA ($pK_a = 4.69$). The swelling in which an increase was observed nearly corresponded to the pK_a value of CA (21).

The efficiency of poly(AAm/CA) hydrogels on removing cationic dye solution is shown in Figure 4.34. The cationic dye molecules interact with the negative charges of poly(AAm/CA) hydrogel, so in the acidic medium the hydrophilic groups of the poly(AAm/CA) do not contain bonded water in the polymer initially, but adsorb water subsequently. According to the protonation of the carboxylic acid groups of hydrogels and amide groups of the dye, at pH 2 and 5 adsorption less than pH 7 adsorption since there is less protonation of amide groups.